

# An Open-Source User Interface Development for Widely Used Low-cost Spectrometer Designs

Güray Gürkan 

Department of Electrical and Electronics Engineering, Istanbul Kültür University, Istanbul, Turkey

**Cite this article as:** Gurkan G. An Open-Source User Interface Development for Widely Used Low-cost Spectrometer Designs. *Electrica*, 2020; 20(2): 133-142.

## ABSTRACT

In this study, the development and test stages of an open-source user interface are presented. The developed user interface is compatible with most of the low-cost camera-based spectrometer designs in the literature. The spectrum image of the light source acquired with the camera is cropped and analyzed in a real-time thread after interactive calibration, which is a special feature of the user interface. Camera controls (e.g., brightness, contrast, saturation, and exposure) are available through the user interface. For user interface testing, a common spectrometer design, which has a light-guide tube with a narrow entrance slit in one end and an image sensor on the other, is constructed. Various compact fluorescent lamps and light-emitting diodes are used as light sources and the results are presented here. Advanced cross-platform user interface can be used with inexpensive spectrometer designs, especially involving a web camera.

**Keywords:** Grating material, image processing, open source, Python programming, user interface design

## Corresponding Author:

Güray Gürkan

## E-mail:

g.gurkan@iku.edu.tr

**Received:** 03.03.2020

**Accepted:** 02.28.2020

**DOI:** 10.5152/electrica.2020.20018



Content of this journal is licensed under a Creative Commons Attribution-NonCommercial 4.0 International License.

## Introduction

The basic function of an optic spectrometer is to split the incoming light or radiation into its sub-components or waves with different wavelengths, and monitor the wavelength peaks for further analysis. Spectrometry, which is used in a larger electromagnetic spectrum rather than the visible spectrum, has various application areas including chemistry (used as mass spectrometry), astronomy, and health. Previously, spectrometers were used as a prism and as a slit. Now-a-days, diffraction-grating materials are used rather than prisms to split incident light into different colors or split into waves with different wavelengths. Depending on the geometrical shape of the material, the incident light can be split into different color lines at a specific distance. Grating materials are recognized by small gaps between the parallel lines. The distance between gaps determines the type of grating material in terms of lines per millimeter, e.g., if a grating gap is 2  $\mu\text{m}$ , the grating material has 500 lines per millimeter.

Because most commercial optical spectrometers are expensive, especially for a self-funded research work and teaching institute, there have been various efforts for developing inexpensive spectrometers. In 1996, Thompson prepared an easy-to-make spectrometer with a possible resolution of 5 nm. He used a long strip of card and then scored the card, folded, and glued around two polystyrene side supports. The document presents the design of the steps for students to directly observe and understand Hg lines in fluorescent lights, the prominent solar Fraunhofer lines, and the spectra of high pressure and low pressure sodium lamps [1]. A plastic holographic diffraction grating (with 750 lines per millimeter) in one side and a slit adjacent to a printed wavelength scale on the other are used for this sensor-free design. Hence, the accuracy of the spectrometer directly depends on the care given through steps of cutting and gluing of the components.

The grating material can be of reflection (mirror) or transmission type in spectrometer designs. Compact-disc (CD) or digital versatile disc (DVD) materials are proposed as transmission type diffraction grating in inexpensive realizations [29].

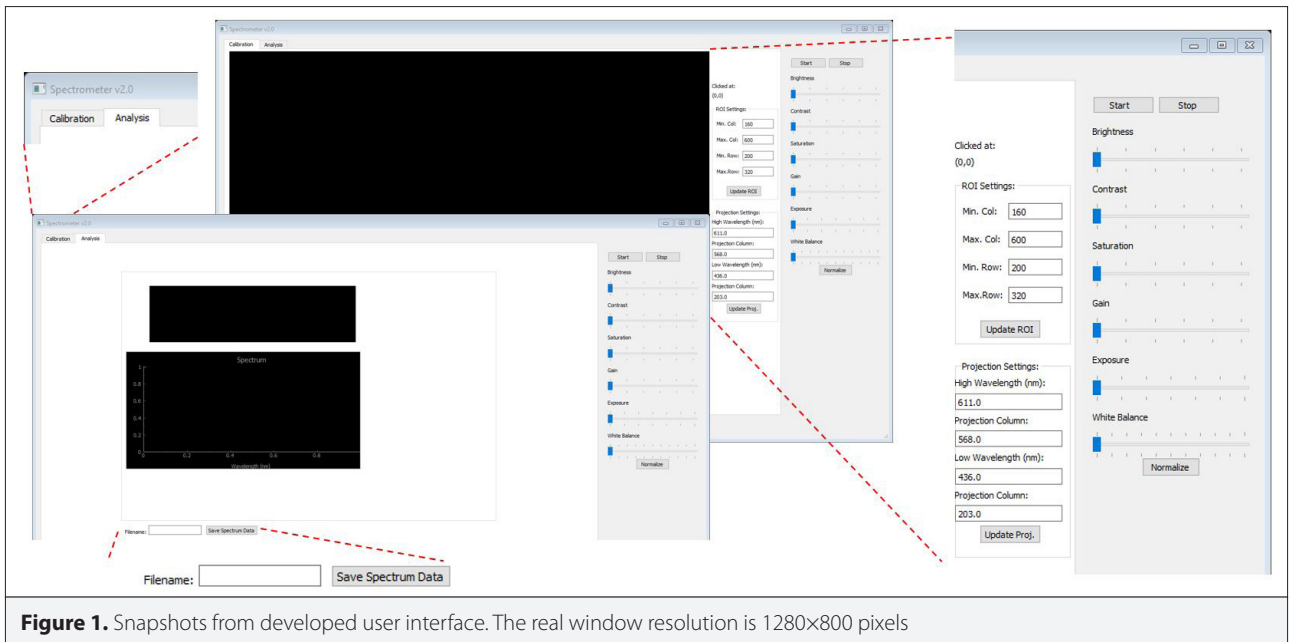


**Figure 1.** Snapshots from developed user interface. The real window resolution is 1280×800 pixels

The diffracted light from reflectance or transmittance grating of a spectrometer is projected on to a sensor. In former designs, the sensor was commonly a photodetector [3]. In such designs, the monochromatic radiation can be measured by rotating the grating material or the sensor to capture the diffraction pattern (e.g., 400–700 nm band in visible band spectrometers). The projected wavelength and the rotation angle should be matched for proper reading. The latest designs use the complementary metal oxide semiconductor (CMOS) type or charge-coupled device (CCD) type sensor arrays (e.g., in video cameras and barcode readers) to capture the entire diffraction pattern without any need of rotation. Most of the recent low-cost spectrometer realizations use universal serial bus (USB) cameras (e.g., web cameras of various brands), on-board programmable cameras (e.g., Raspberry Pi camera, Raspberry Pi Community, UK), or smartphone cameras for capturing the diffracted light pattern.

McGonigle et al [8] published a comprehensive review of various architectures, application areas, and future challenges of smartphone spectrometers. Hobbs et al. [9] built five distinct spectrometer designs. They tested the spectrometers for absorption using concentrations of fluids and for reflectance using color swatches and various minerals. The grating material used was a DVD diffraction grating in three designs. Camera, such as Raspberry Pi camera, 700 lines monochromatic CCD camera, and ZWO AS1034MC astronomical camera (Suzhou Zwo Co., Ltd., Suzhou, China) used sensor and tungsten photo lamp as the light source. The remaining two designs did not even use a diffraction grating. They used monochromatic sensor (photodiode) and single color light source.

Recent studies on low-cost spectrometer realization primarily focus on hardware construction (e.g., 3D printing, reflectance–transmittance modes, and the sensor selection). The acquired

spectrum image should be first calibrated in camera-based spectrometers. Each diffracted monochromatic components (e.g., wavelength) of the incident light is projected onto a different pixel location. Generally, a light source with a known spectrum (preferably with spectral lines or specific spectral peaks) is used for calibration by which pixel locations can be matched to corresponding wavelengths. After calibrating the image, captured (and unknown) spectrum images can be properly described. However, if any hardware changes (e.g., tube length or focus length of the lens, grating line number) are made or any small deviations (e.g., positioning of sensor, grating material, or even light source) occur, the calibration process should be repeated. Most of the images are processed offline by third party [2, 5, 8, 9] or by using developed [4, 6] applications causing impractical and error-prone measurements.

In this study, a Python-based open-source user interface (Figure 1) enabling real-time (online) interactive calibration and spectral measurement that can be used for all camera-based designs for spectrometer is presented. The software is tested for Windows, Linux, and Raspbian platforms.

In this study, the construction of a (test) design for spectrometer has been described [9, 10]. The experiments for measuring grating dispersion and emission wavelengths of lasers that are used in calibration of the spectrometer (software) has been demonstrated. The different features on developed user interface are presented in detail along with the details of further tests and results

### The Realization of the Test Device

The test device comprises grating material and its holder, the slit, and a box for housing the web camera. The box is recognized by Plexiglas material. A narrow (600 μm × 10 mm) slit lo-

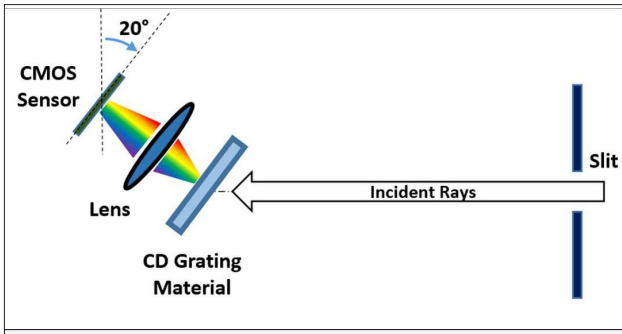


**Figure 2.** Illustration of incident light projection through tested spectrometer design

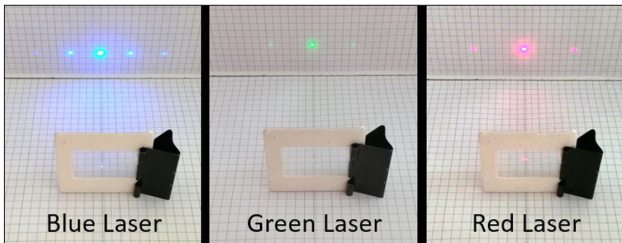


**Figure 3.** Modes of diffraction obtained for 500 lines/mm grating material. The distance between grating material and projection surface is 100 mm in each test

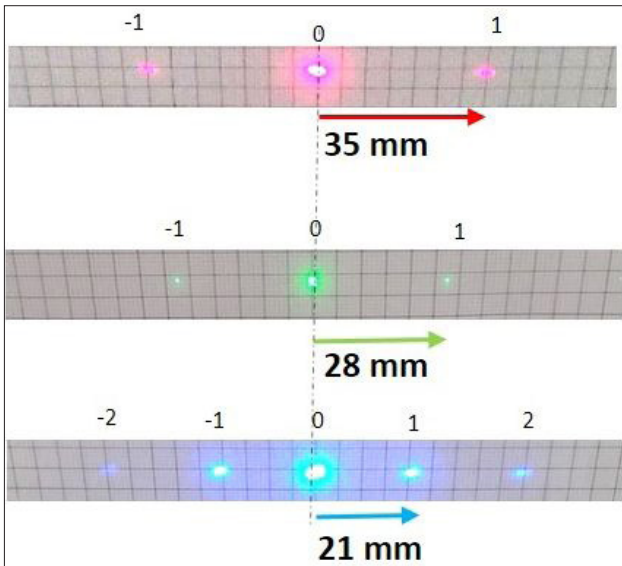


**Figure 4.** Zoomed projections obtained for each laser source. The distance between grating material and projection surface is 100 mm in each test. Visible grid length is 5 mm

cated on the aperture side of the box and is realized using two razor sharps. To absorb non-parallel incoming rays, the inner side of the box is covered with non-reflective material. In front of the USB web camera with a CMOS image sensor (Logitech C270 USB Web Camera, Logitech International S.A., Lausanne, Switzerland), the CD grating material is placed.

The selected web camera can capture up to 30 colored frames per second (fps) with a resolution of  $1024 \times 768$ . To get a larger projection size, the web camera's fixed lens is replaced by an S-mount lens with focus length of 10 mm. The S-mount lens has a metric M12 thread with 0.5 mm pitch size and was detached from an analog camera. Manual focusing can be realized by rotating the thread. The slit and camera lens are aligned in vertical position and the horizontal camera orientation (Figure 2) is adjusted to  $20^\circ$ . The slit is invisible in captured image in this state. The details of the camera orientation are given in the next section.

### Measurement of Laser Wavelengths and Grating Parameter

If the relation between the pixel position and wavelength is known, any spectral image can be converted to a meaningful wavelength scale. To obtain the relation between the pixel position and wavelength, the observer must first take a spectrum with known wavelengths and then calibrate the pixel scale into wavelength [4]. Author selected some commercially available low-power (<5 mW), dot beam-shaped laser sources with red, green, and blue colors to have known wavelengths for calibration of the developed spectrometer. The manufacturer provided the emission wavelengths as  $405 \pm 10$  nm for blue laser,  $532 \pm 10$  nm for green laser, and  $650 \pm 10$  nm for red laser, respectively.

### Measurement of laser wavelengths

An experiment setup with a grating material with 500 lines/mm parameter is constructed to measure the wavelength of true emission of each laser source using a low-cost method. A transmission diffraction grating with a known number of lines per millimeter can be used to measure the wavelength of emission of a laser source. If the grating material is placed at a definite distance from a projection surface, directed laser will split into a pattern of multiple points, called the (maximum) modes of diffraction. As the spot size of the lasers is larger than 1 mm, 1 mm  $\times$  1 mm grid paper can be used for measurements. So, the projection readings are limited to 1 mm resolution. Before taking the printout, the major (bold) grid size is adjusted to 5 mm  $\times$  5 mm.

Figure 3 shows the projections obtained from three lasers and the detailed analysis of projections are given in Figure 4. The first mode distances are measured as 21 mm for blue laser, 28 mm for green laser, and 35 mm for red laser, respectively. The incident rays that arrive normal on the grating surface are not diffracted. Instead, these are transmitted with higher intensity levels. As the rays of higher modes are diffracted, they have relatively lower intensity. In each mode, the red laser has the highest diffraction angle. The diffraction angle can be calculated by the following relation:

$$\theta = \tan^{-1}(x/D) \quad (1)$$

where  $x$  is the distance between the middle ray and the first order projection,  $D$  is the distance of grating to a projection surface,  $\theta$  is the diffraction angle,  $\lambda$  denotes the laser wavelength, and  $d$  (which is 1/500 mm for our case) represents grating line spacing. The relation between  $\lambda$  and  $d$  are shown by Equation (2).

$$d \sin \theta = \lambda \quad (2)$$

Thus, using trigonometric identities and Equations (1) and (2), the emission wavelength can be calculated as

$$\lambda = d \sin(\tan^{-1}(x / D)) = \frac{d \cdot x}{\sqrt{x^2 + D^2}} \quad (3)$$

In the experiments, grating material to projection distance,  $D$ , was fixed at 100 mm. Thus, the wavelength for blue laser emission is calculated as 405 nm, the wavelength for green laser emission is calculated as 539 nm, and the wavelength for red laser is calculated as 660 nm (Table 1). The wavelength of green laser emission coincides with the known emission wavelength of diode-pumped solid state neodymium yttrium aluminum perovskite (DPSS Nd:YAP) type lasers [11].

### Measurement of CD Grating Line Gap

After experimental calculation of the laser emission wavelengths, the experiment for determination of CD grating line gap is comprehended. For this, grating material is replaced by a CD grating and the first mode diffraction distance, denoted by  $x$  in Equation (1), for green laser (539 nm) is measured. The distance is found to be 40 mm. Substituting  $x=40$ ,  $\lambda=539$ ,  $D=100$  in Equations (1) and (3), we get  $\theta=21.8^\circ$  and  $d=1.45 \mu\text{m}$  as line gap (or 688 lines/mm). As the wavelength of the green laser is very nearly located in the middle of the visible spectrum, diffraction angles for the entire visible spectrum will be symmetrical around  $\sim 20^\circ$  for CD grating material. That is the reason behind the rotation choice of grating material and camera sensor in the hardware design (Figure 2).

The diffraction angles and the focus length of the lens determine the location of the spectral component projections on the image sensor. Incident rays those are arriving normally on grating material are not diffracted, and that causes an over-exposed image of the slit area. The first mode diffractions of incident rays build the first and the brightest spectrum of the input source. However, if both the first mode-diffracted rays and the normal rays are projected on the image sensor, the image will be dominated by over-exposed slit image. As a result, the spectrum will be lost. In addition, the increased gap between the grating material and lens decreases the projection area. Therefore, the CD grating material and the camera are closely located

**Table 1.** Measurement Results and Calculated Laser Emission Wavelengths for 500 Lines/mm Grating (Grating – projection surface distance ( $D$ ) is 100 mm)

Laser	1 <sup>st</sup> Mode Distance	Diffraction Angle	Calculated Wavelength
Red	35 mm	19.29°	660 nm
Green	28 mm	15.64°	539 nm
Blue	21 mm	11.86°	410 nm

and given a rotation so that the high intensity slit is invisible in the captured image and the green wavelength is located in the middle.

### Developed User Interface and Image Processing Algorithm

The user interface design, processing algorithms, and real time image acquisition are developed using the platforms of Python (Python Software Foundation) and Qt-Designer (The Qt Company, Helsinki, Finland). The user interface (Figure 1) enables the adjustment of (available) camera settings (e.g., exposure, gain, and brightness). The acquired and region of interest (ROI) cropped images and calculated spectrogram are displayed in the “Analysis” tab of the user interface.

The user interface is developed using Qt-Designer and is saved in (\*.ui) file format. This format cannot be directly embedded in a Python environment. By using “pyuic4” command in PyQt4 library, the designed user interface can be converted first to a (\*.py) file and then merged to a Python application. The main Python application Python 2.7.10 is developed. Image acquisition and camera control algorithms are developed using Python’s OpenCV, PyQt, and Pyqtgraph (MIT Labs, USA) libraries. For plotting high frame rate graphs, Pyqtgraph is a powerful Python library.

The most important capability of the developed software is that it enables the user to configure ROI area and provides the projections of the values of the wavelength from scratch using “Calibration” tab. For any visible band spectrometer design that consists of a OpenCV compatible camera, this user interface can be used.

### Interactive Region of Interest Selection

The acquired image has 1024 × 768 pixel size with 8 bits of resolution in red, green, and blue (RGB) color channels. So, an interactive algorithm is developed to determine the limits of the projection in a hardware independent manner.

After initiating real-time image capturing by pressing “Start” button, user should switch to “Calibration” tab. For proper calibration of the projection area, the spectrometer should be directed to daylight or simply through the noon sky, which ideally involves the entire visible spectrum. The spectral response of the CMOS sensor along with the infrared- and ultraviolet-re-

**Figure 5. a, b.** Interactive ROI (a) and projection adjustment (b) widgets located in Calibration tab of the developed user interface

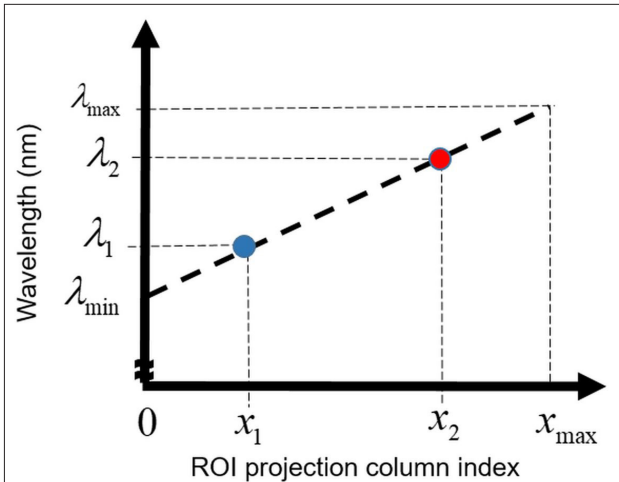


**Figure 6.** Linear mapping from projection column indices to wavelengths

jecting optical filter on the camera lens restricts the projection area to a specific pixel area.

While the projection is visible in the entire  $1024 \times 768$  image, the user can click on the left mouse button to update “Clicked at:” label for each ROI rectangle pixel coordinates. Then, they can enter the proper “Line Edit” widgets (Figure 5a). The “clicked” pixel coordinate is only refreshed only when a new left click occurs.

After new ROI coordinates are entered, the user can save these in a text file (“roi\_settings.txt”) by pressing “Update ROI” button. These settings are automatically reloaded from the same file after starting the next program.

### Interactive Projection Calibration

After determining ROI, projected column pixel locations should be matched to corresponding wavelengths. In the same way, the user can interactively able to configure projections. For this, user should have at least two spectral peaks with known wavelengths. In the literature, it is common to use compact fluorescent lamps (CFLs). However, the spectrum peaks may vary across different brands [12]. For this problem, the author proposes two lasers with known wavelengths for emission.

The user may first apply laser with higher or lower wavelengths. For example, if laser with lower wavelength is applied to the slit, user should first left click on the projected laser beam location of the entire image, note the pixel column value, and then enter this value in the corresponding “Projection Column” (Figure 5b). Afterward, the user should repeat the same process for applying the laser with a higher wavelength. The gain and exposure parameters should be carefully adjusted to ensure the narrowest projection yielding to best focus and most sensitive detection. The value of the wavelengths should also be entered into the corresponding LineEdit widgets. Finally, the user should complete the projection calibration process by pressing “Update Proj.” button. Similar to ROI settings, these parameters are saved in a separate text file named “projection\_settings.txt”.

### Projections to Wavelengths

The developed algorithm considers a linear mapping [46] between wavelengths and projections as

$$\lambda_i = ax_i + b \quad (4)$$

where  $a$  is the slope of the mapping line (in nm/column),  $x_i$  is the ROI projection column index of the projected wavelength  $\lambda_i$ , and  $b$  is the offset value (Figure 6). In fact, parameter  $b$  is the smallest value (ideal) of the wavelength that can be detected by the spectrometer.

In interactive projection calibration mode, the calibration pairs  $(x_1, \lambda_1)$  and  $(x_2, \lambda_2)$  are the values that are entered and saved by the user. By substituting the calibration pairs in Equation (4), values of  $a$  and  $b$  are obtained as

$$a = \frac{\lambda_1 - \lambda_2}{x_1 - x_2} \quad (5)$$

and

$$b = \frac{x_1\lambda_2 - x_2\lambda_1}{x_1 - x_2} \quad (6)$$

By using Equations (5) and (6), the minimum and maximum ideal values of the wavelengths can be calculated as

$$\lambda_{\min} = b = \frac{x_1 \lambda_2 - x_2 \lambda_1}{x_1 - x_2}, \quad (7)$$

and

$$\lambda_{\max} = ax_{\max} + b = a(Col_{\max} - Col_{\min} - 1) + b \quad (8)$$

where  $x_{\max}$  is the maximum value of the projection column index,  $Col_{\max}$  is the maximum, and  $Col_{\min}$  is the minimum column indices of the global ROI pixel coordinates that are entered in interactive ROI selection mode.

### Verification of the Proposed Mapping Method

The spectrometer is directed to noon sky and the parameters are adjusted for calibration (Figure 5a). Blue (410 nm) and red (660 nm) lasers are fed into the spectrometer after configuring the ROI parameters. Projection parameters are interactively adjusted from the images as shown in Figure 5b.

Referring to adjusted ROI and projection settings, the blue (410 nm) laser should be projected to  $241202=39$  ROI column index, whereas the red (660 nm) laser should be projected to  $761202=559$  ROI column index. ROI cropped images in Figure 7a and Figure 7b verify this result. As the projections have more than one column length, the middle column index is selected as the reference for each laser.

Referring to Equations (5) and (6), the mapping parameters are calculated as  $a=0.48077$  and  $b=391.25$ .

The final step of the verification of the linear mapping is to check whether the green laser projection column index and its wavelength are consistent, or not. The obtained ROI cropped image and column index are shown in Figure 7c.

By using the calculated values of  $a$  and  $b$  and the projection index value as 308, the mapped wavelength is calculated as

$$\begin{aligned} \lambda_{\text{mapped}} &= 308a + b \\ &= 308 \cdot 0.48077 + 391.25 = 539.32\text{nm} \end{aligned} \quad (9)$$

Thus, the known value (539.25 nm) of the wavelength of green laser can be calculated from the projection of column index 308 by the linear mapping method. This result verifies that the input wavelengths and linear mapped values are consistent for the visible range.

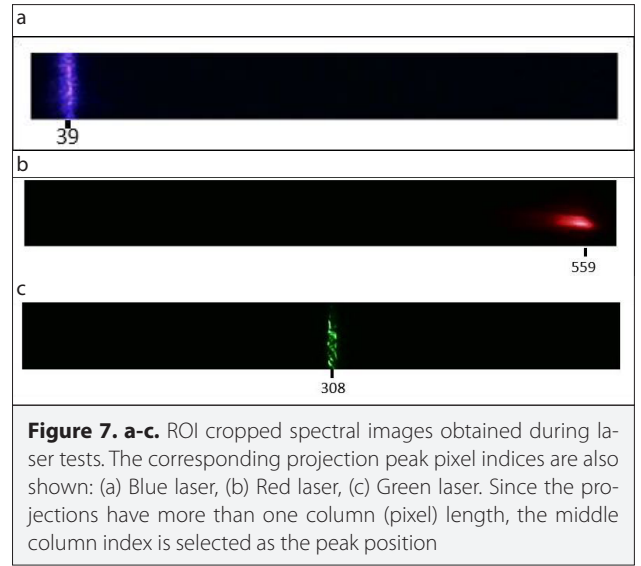


**Figure 7. a-c.** ROI cropped spectral images obtained during laser tests. The corresponding projection peak pixel indices are also shown: (a) Blue laser, (b) Red laser, (c) Green laser. Since the projections have more than one column (pixel) length, the middle column index is selected as the peak position

### Calculation of Spectrum

By applying ROI calibration method, the image size of the cropped RGB image can be determined by the user. For a cropped image matrix with  $N$  rows,  $M$  columns, and 3 RGB channels,  $N$  is equal to the difference between minimum and maximum row indices of the entire  $768 \times 1024 \times 3$  image. Similarly,  $M$  is equal to the difference between the minimum and the maximum column indices. To obtain the spectrum vector, RGB image is first summed through its channels, yielding to an  $N \times M$  matrix. Afterward, this "cumulated intensity" image is summed up through its rows, yielding a spectrum vector with  $M$  elements. So,

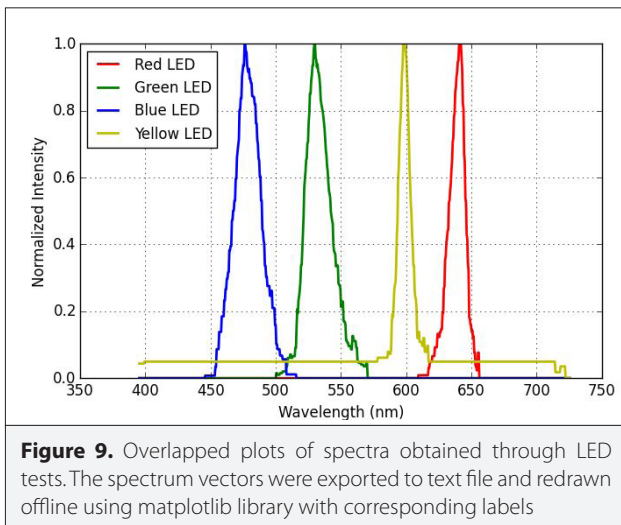
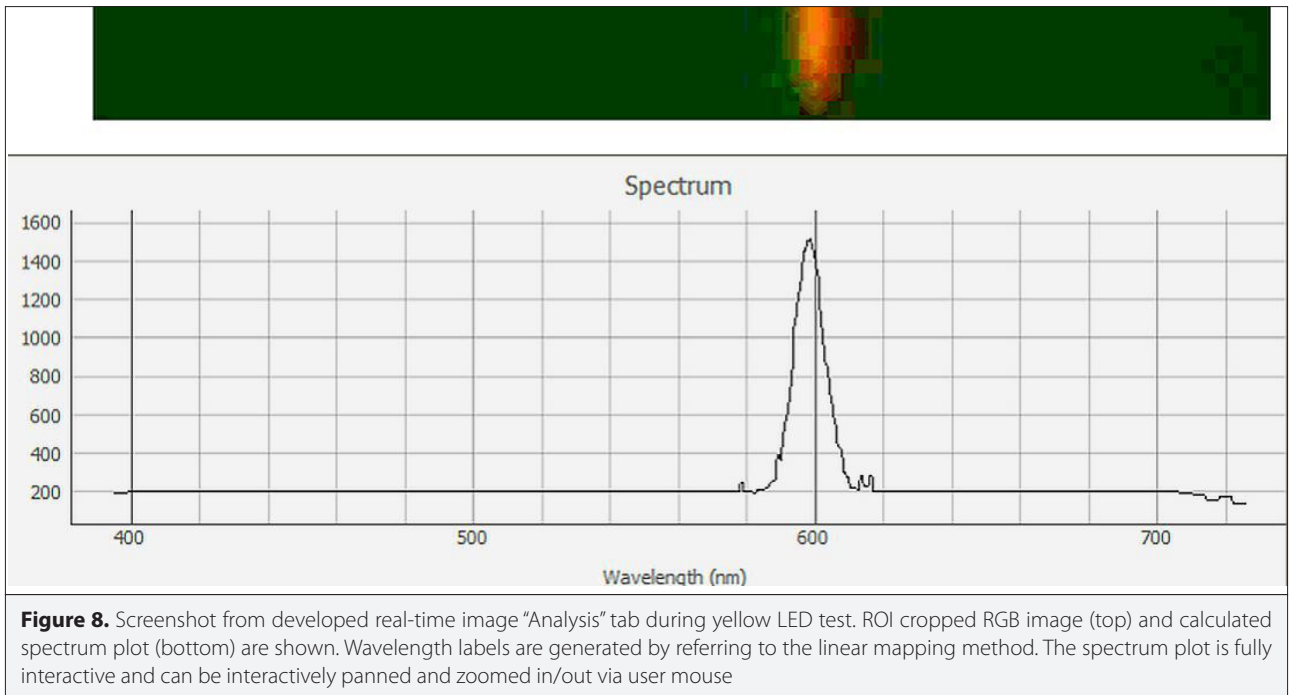
$$S(c) = \sum_r I(r, c), \quad c = 0, 1, \dots, M - 1 \quad (10)$$

where  $I$  is the cumulated intensity image,  $r$  is the row index, and  $c$  is the column index of the image.

The resulting spectrum vector and calculated wavelength labels are plotted in the "Analysis" tab of the developed graphical user interface (GUI). This process is repeated in every 100 ms to obtain a (arbitrary) refresh rate of 10 Hz. The refresh rate can be increased up to native frames per second (fps) rating of the camera. Real-time plotted spectrum with wavelength values and corresponding amplitudes can be exported to a text file by pressing "Save Spectrum Data" button (Figure 1).

The interpretation of intensity-based amplitudes in the spectra is beyond the scope of this study. However, one should note the following points:

(a) RGB CMOS sensor uses Bayer filter structure. Thus, in every  $2 \times 2$  pixel area, number of green pixels is twice that of the blue and red pixel numbers. This yields unequally weighted intensity measures for different wavelengths.



(b) CMOS spectral response is unknown.

(c) Absorbance parameters of diffraction-grating materials and lens should also be measured.

The developed algorithm deals only with the accuracy of wavelength mapping. Thus, the spectrum vector can be simply obtained by summation through RGB channels of the ROI cropped image.

### Tests and Results

As the first step of tests, light-emitting diodes (LEDs) and indoor compact florescent lamps (CFLs) are used as light sources. The software is run on a computer with 64-bits Windows 10 OS,

Intel Core I5 4210 1.7 GHz CPU, 8 GB RAM, and Intel HD Graphics Card. Python 2.7 and required modules (Numpy, Matplotlib, Pyqtgraph, OpenCV) were already installed on the host computer.

Four colors of LEDs (red, yellow, green, and blue) are used under identical capture parameters (exposure, gain, saturation, contrast, and brightness). Moreover, light intensities are adjusted by controlling the input current of LEDs so that the cumulated intensity is close to (an arbitrary value of) 2000.

A screenshot captured from the developed user interface during the yellow (orange) LED test is shown in Figure 8. This figure shows two plots: the top plot shows the results of the cropped web camera RGB image and the bottom plot shows the calculated spectrum. Both the plots are refreshed in every 100 ms with a timer thread. The x-axis range of the spectrum plot is 392729 nm for the current calibration, but the plot can be interactively panned and zoomed in/out via user mouse. The spectrum plot in any frame can be exported as a text file or picture using developed user interface. A detailed analysis of the LED spectra reveals that the peak wavelength for blue LED is 476 nm, for green LED is 530 nm, for yellow (actually orange) LED is 598 nm, and for red LED is 641 nm, respectively.

The spectrum with a single peak is obtained in single colored LED test. The peak location directly depends on the type of the inorganic semiconductor material of the LED. For example, a gallium arsenide phosphide (GaAsP) type LED may have an orange or red color depending on the doping ratio. From corresponding text files, exported spectrum data of four LED measurements were loaded and redrawn using ‘matplotlib’ Python library to validate exported data (Figure 9).

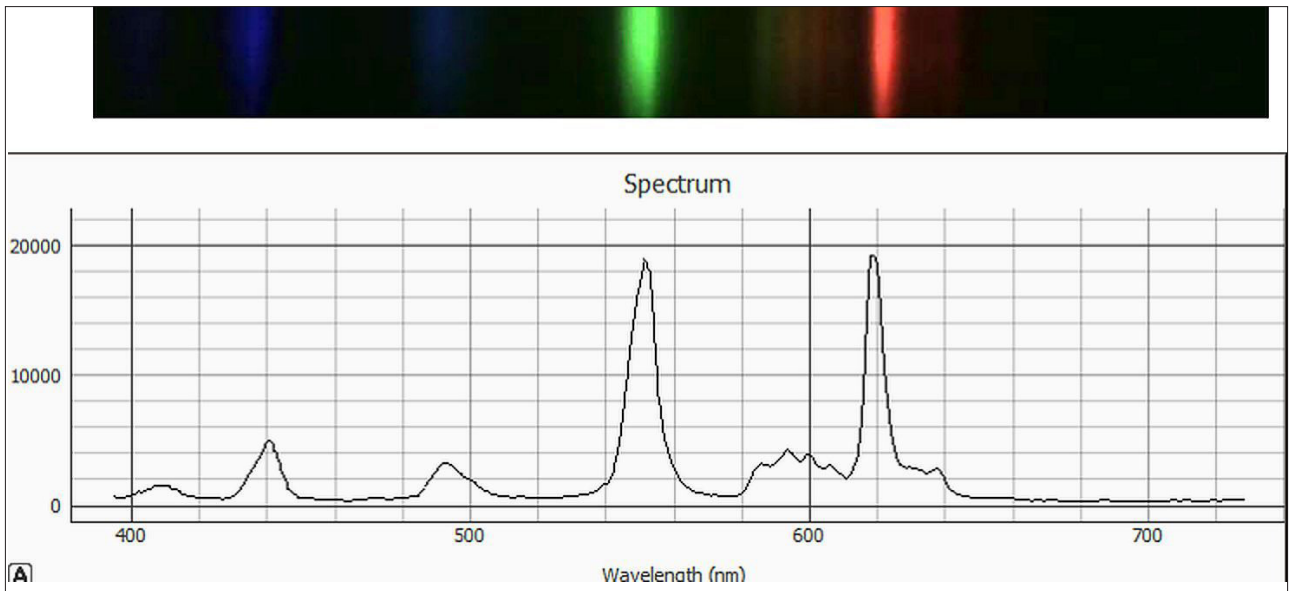


**Figure 10.** Screenshot from 2700K – 15W CFL test

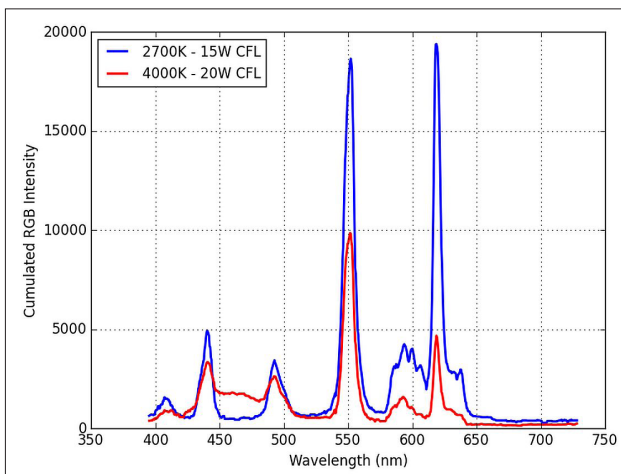


**Figure 11.** Overlapped plots of exported CFL spectra data via "matplotlib" Python library. Darkness intensity level is consistent due to identical capture parameters adjusted during two CFLs

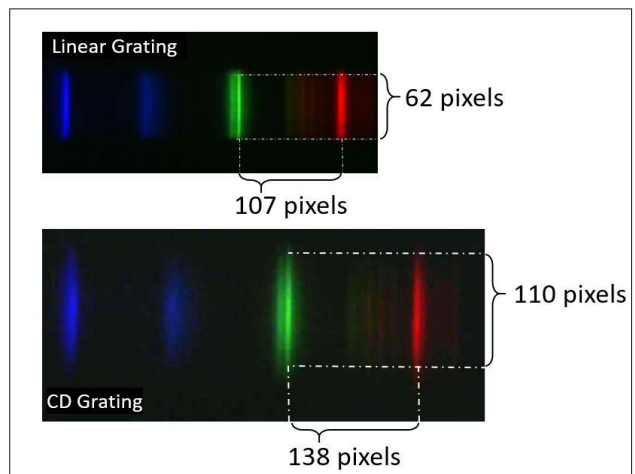


**Figure 12.** Performance of the user interface calibration feature via comparison of linear and CD grating material generated spectrums for 2700K CFL test

**Table 2.** Measured vs. standard spectrum peaks of CFLs and origin materials

Color	Origin	Peak	Measured
Dim violet	Mercury	404	408
Dim blue	Mercury	436	440
Turquoise	Terbium	485 490	492
Green doublet	Terbium and Mercury	544 546	551
Red	Europium	611	618

Unlike single colored LEDs, CFLs involve more than one spectral peak with known emission wavelengths [12]. Referring to these values, two CFLs (Philips Economy Energy Saver 20 W 4000 K and Philips Economy Twister 15 W 2700 K) are tested under identical capture parameters. A screenshot of the results from the developed user interface during the CFL test is shown in Figure 10. For a detailed analysis of the spectral peaks, exported spectrum data are replotted offline through matplotlib library (Figure 11). The detected peak locations (Table 2) represent that the developed system can measure CFL peaks with a considerable error (i.e., <5 nm) due to the wide spot size (>1mm) of the lasers that are used for calibration.

To demonstrate the consistency and flexibility of the user interface for a different spectrometer configuration, CD diffraction grating has been replaced by a 500 lines/mm linear grating, which alters the row-column pixel width of the diffracted spectrum on the camera sensor. After replacement, spectrometer can be interactively re-calibrated under the noon sky and (any two of) using the same laser sources.

For comparison, the spectra of 2700 K CFL was used (Figure 12). The CD grating has a larger number of lines per millimeter (~644) in comparison to the linear grating (500). This causes a larger diffraction, which results in more distant spectral peaks and enlarged ROI. This problem can be solved in calibration mode. Moreover, CD grating causes loss of higher intensity. Therefore, it needs higher exposure and gain settings to be adjusted for proper capturing of the spectrum, which can also be easily adjusted through the corresponding user interface sliders in real-time.

### Conclusion

The existing open-source and cross-platform user interface can be used for preparing low-cost designs for spectrometer. Further developments in the user interface may also facilitate absorbance spectrum calculations attended with proper spectrum hardware.

**Peer-review:** Externally peer-reviewed.

**Acknowledgment:** Project source files can be found at the author's Github page.

**Conflict of Interest:** The authors have no conflicts of interest to declare.

**Financial Disclosure:** The authors declared that the study has received no financial support.

### References

1. K. Thompson. "An easy-to-build spectroscope". *Physics Education*, vol. 31, no. 6, pp.382-385, 1996. [\[Crossref\]](#)
2. S.F. Tonkin, "Practical Amateur Spectroscopy", 2nd Edition, Springer-Verlag London Limited, 2004.
3. G. Veras, E. C. Silva, W. S. Lyra, S. F. C. Soares, T. B. Guerreiro and S. R. B. Santos. "A Portable, Inexpensive and Microcontrolled Spectrometer Based on White LED as Light Source and CD Media as Diffraction Grid." *Talanta*, vol. 77, no. 3, pp. 1155-1159, 2009. [\[Crossref\]](#)
4. E. Widiatmoko, M. B. Widayani, A. Mikrajuddin, and Khairurrijal. "A Simple Spectrometer Using Common Materials and A Digital Camera.", *Physics Education*, vol. 46, no. 3, pp. 332-339, 2011. [\[Crossref\]](#)
5. KR Shailesh, CP Kurian and SG. Kini. "Auto-calibration of emission spectra of light sources captured using camera spectrometer", *International Conference on Smart Sensors and Systems (IC-SSS)*, 2015, pp. 1-5. [\[Crossref\]](#)
6. F. Wakabayashi. "Resolving Spectral Lines with a Periscope-Type DVD Spectroscope", *Journal of Chemical Education*, vol. 85, no. 6, pp. 849, 2008. [\[Crossref\]](#)
7. F. Dominec, "Design and construction of a digital CCD spectrometer", Research Project, Department of Physical Electronics, Czech Technical University, 2010.
8. AJ McGonigle, TC Wilkes, TD Pering, JR Willmott, JM Cook, FM Mims, AV Parisi. "Smartphone Spectrometers", *Sensors* vol. 18, no. 1, pp. 223, 2018. [\[Crossref\]](#)
9. S. W. Hobbs, D. J. Paull, T. McDougall. "Evaluating low-cost spectrometer designs for utility in reflectance and transmittance applications", *International Journal of Remote Sensing*, vol. 40, no. 2, pp. 642-669, 2020. [\[Crossref\]](#)
10. Y. Cai, *Ambient Diagnostics - Chapter 12: Personal Spectrometers*, CRC Press, 2014. [\[Crossref\]](#)
11. H. Bjelkhagen, D. Brotherton-Ratcliffe. *Ultra-Realistic Imaging: Advanced Techniques in Analogue and Digital Colour Holography*, CRC Press, 2016. [\[Crossref\]](#)
12. M. Khazova, JB O'Hagan. "Optical radiation emissions from compact fluorescent lamps", *Radiation Protection Dosimetry*, vol. 131, no. 4, pp. 521-525, 2008. [\[Crossref\]](#)



GÜRAY GÜRKAN received his B.Sc. degree in Electronics Engineering from Istanbul University (Istanbul, Turkey) in 2003 and Ph.D. degree in Biomedical Engineering from Istanbul University in 2011. Since 2012, he has been working as an Assistant Professor in Istanbul Kültür University, Istanbul, Turkey. His current research interests include embedded systems, real-time signal processing, biomedical instrumentation, data acquisition and visualization, user interface development and open-source software development.